2009 American Control Conference
Hyatt Regency Riverfront, St. Louis, MO, USA
June 10-12, 2009

Vehicle Pure Yaw Moment Control Using Differential Tire Slip

Wei Liang, Hai Yu, Ryan McGee, Ming Kuang, Jure Medanic

Abstract— **Direct yaw moment control generated by differential friction forces on an axle has been proved to be effective in improving vehicle lateral yaw stability and in enhancing handling performance. It consists of two levels of control tasks: calculating a yaw moment command at vehicle level and regulating the tire slip to deliver the moment at wheel level. Advanced powertrain with electrical in-wheel-motor makes fast wheel level control possible. This paper proposes an adaptive tire slip controller for Pure Yaw Moment Generation, which yields the maximal axle yaw moment by asymmetric axle friction force with no effect on vehicle longitudinal speed. Since the maximal friction is limited by the tire-road contact, control constraints at various vehicle speeds and on different surface conditions has to be taken into account. This algorithm can generate the optimal longitudinal slip ratio at the presence of lateral tire force based on a 2D Modified-LuGre tire model. One major difficulty of such type controllers is the unknown surface condition. A nonlinear adaptive braking/traction torque control is proposed to regulate the tire slip ratio with the estimation of surface condition. Simulation studies show that feeding back the estimate into the slip control makes the delivered friction force and yaw moment adaptive to surface conditions.**

I. Introduction

Advanced chassis technology using Direct Yaw Moment (DYM) generated by differential friction forces of the left and right side of a vehicle has been implemented in Electronic Stability Control (ESC) systems. ESC has shown significant effect on improving vehicle lateral stability. Most of studies on DYM design reported in literature [1], [2], [3], [7], [8] have focused on vehicle level yaw moment regulation. Current ESC implementations use either brake-based or traction-based differential friction forces to generate the desired yaw moment. Innovative powertrain technologies provide additional freedom of utilizing DYM. In-wheel-motor electric drive is a type of advanced powertrain system that can be used in future hybrid and fuel cell vehicles. Each axle contains two independent wheel motors and each machine can work as either a driving motor in normal drive or a generator in regenerate braking. The fast response of the electric motors make it possible to use brake-traction-based DYM control. In such a case, the motor on one side of the axle will work in motoring mode to generate longitudinal traction force and the other one will work in regenerating mode to provide a brake force in the opposite direction. Such type approach can maximize the usage of the available friction force since it ideally can double the moment generated by brake-based or traction-based ESC systems.

This work was partially finished when Wei Liang was a graduate student at the University of Illinois at Urbana-Champaign. Wei Liang, Hai Yu, Ryan McGee and Ming Kuang are with Ford Motor Company at 15000 Commerce Dr. N, Dearborn, MI 48120, wliang3@ford.com, hyu20@ford.com, rmcgee3@ford.com, mkuang@ford.com

Jure Medanic is Emeritus Professor of Department of Industrial and System Engineering at the University of Illinois at Urbana-Champaign.

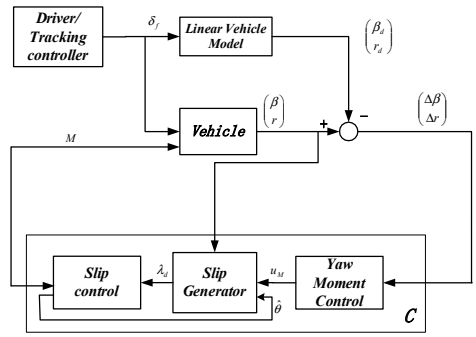

Fig. 1. Diagram for wheel slip control

Real-time wheel slip control for DYM is difficult given the fact that no practical real-time measurement is available for surface friction condition. It is highly desirable for the control algorithm to determine and generate an optimal yaw moment on a wheel-tire system for any given physical surface condition. In [6], the vehicle stability control problem that can use maximum available DYM has been formulated as a multiple-layer control problem as shown in Figure 1. Yaw Moment Control is a vehicle-level controller determining the yaw moment command satisfying vehicle yaw stability request. It yields a command u_M to the lower level wheel/tire controller. The lower level controller is composed of two parts: Slip Generator and Slip Controller. The Slip Generator computes the optimal slip ratio λ_d which maximizes the yaw moment for a nominal surface condition when the maximum of u_M is commanded. This determination takes into account the tire lateral deflection. It has been found that the optimal slip ratio for direct yaw moment generation is not the one achieved by current ABS systems, which is the one delivering the maximal longitudinal friction force. The Slip Controller regulates the tire slip ratio λ to the desired quantity λ_d by using the braking/traction torque T on the wheel as the control actuator. The design generated a Pure Yaw Moment (PYM) controller. It delivered equal friction forces on two sides of the axle with opposite directions so it has no impact on vehicle speed. From this perspective, it is the ideal DYM controller.

One obstacle for the implementation of PYM on current vehicle platforms is the difference in response time between the braking system and the powertrain dynamics. This difference makes it challenging to maintain the asymmetric

slip ratio. Advanced electric vehicle powertrain with an in-wheel-motor axle solves the problem. In [10], a vehicle level Independent Torque Biasing (ITB) control has been designed to assist steering and to improve vehicle yaw stability by using the LQG control method.

This paper uses a PYM controller for the ITB Torque Arbitration in slip Control and surface condition estimation. Section II gives a brief introduction to the Modified-LuGre tire model used in this study. Section III calculates the optimal slip ratio when taking into account the 2D effect of tire friction in generating a yaw moment. A Lyapunov function based adaptive control design which identifies the surface condition and regulate the tire slip ratio is given in Section IV. The identified surface condition parameter will be sent back to the slip generator to adjust slip command. It is an optimal tire traction control, which incorporates tire traction limits for each wheel. Section V presents the simulation results of the designed controller and Section VI is the conclusion from the study.

II. Modified-LuGre Tire Friction Model

The nonlinear brake/traction tire slip control in this study uses a Modified-LuGre tire model. It is developed in [5] with a lumped parameter form which captures the transient of the average dynamics of the tread bristles and a steady state form which represents the tire tread deflection with the generated friction force in the steady state. The dynamic lumped parameter model has the form of a first order partial differential equation with an unmeasurable state and it is used in control design. The steady state model can be compared with empirical models and tire test data for the purpose of model correlation and parameter fitting. In [5], a new form of two-dimensional tire friction model is also introduced which is used in this study for yaw moment generation at the presence of 2D tire deflection.

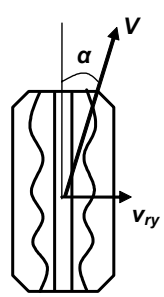

Fig. 2. Wheel velocity and tire slip speed (top view)

The 2D tire slip velocities are shown in Figure 2 for a wheel planetary velocity V and rotational speed ω. The tire-road relative slip velocities in the two directions are $v_{rx} = V\cos(\alpha)\lambda$ and $v_{ry} = V\sin(\alpha)$, $v_r = \sqrt{v_{rx}^2 + v_{ry}^2}$, $V_x = V\cos\alpha$ and $V_y = V\sin\alpha = v_{ry}$. α is the tire side slip angle and λ is the longitudinal slip ratio, $\lambda = v_{rx}/V_x = (V_x - rw)/V_x$ for the braking case.

The 2D model used in maximum yaw moment control has to capture the effect of λ on the friction force in Y direction F_y. In this study, a 2D modified-LuGre tire friction model with the form

$$F_i = F_n[\frac{\mu_{ki}^2 v_{ri}}{\gamma(v_r,\mu)}(1 - \frac{\beta}{a_i^2}(\frac{e^{-a_i L_t} - e^{-a_i(L_t-\zeta_L)}}{\zeta_L} - \frac{e^{-a_i(L_t-\zeta_R)} - 1}{L_t - \zeta_R})) + \sigma_2 v_{ri}] \quad (1)$$

is used, where $i = x, y$. It is a steady state friction model coupling longitudinal and lateral friction, with

$$\mu_{kx}(v_r) = \mu_{cx} + (\mu_{sx} - \mu_{cx})e^{-\left|\frac{v_r}{v_{sx}}\right|^{1/2}} \quad (2a)$$

$$\mu_{ky}(v_r) = \mu_{cy} + (\mu_{sy} - \mu_{cy})e^{-\left|\frac{v_r}{v_{sy}}\right|^{1/2}} \quad (2b)$$

$$\gamma(v_r) = \sqrt{(\mu_{kx}v_{rx})^2 + (\mu_{ky}v_{ry})^2}$$

and $a_i = \frac{\hat{\sigma}_{0i}\gamma(v_r,\mu)}{\mu_{ki}^2(v_r)rw}$, $\beta = \frac{2}{L_t+\zeta_R-\zeta_L}$. μ_{cx}, μ_{cy} are the Coulomb friction coefficients and μ_{sx}, μ_{sy} are the static friction coefficients of the contact in $x-$ longitudinal and $y-$ lateral direction. Equation (2a) and (2b) describes the Stribeck effect of friction at different sliding speeds with respect to the surface. The 2D tire model (1) uses some common parameters for the longitudinal and the lateral direction. The common tire parameters are the length of the tire-ground contact patch $L_t = 0.2$, the parameters of the load shape function $\zeta_L = 0.09$, $\zeta_R = 0.12$. Model (1) can predict 1D/2D steady state tire friction with good accuracy. The details of the tire model with fitted model parameter can be found in [5].

The steady state model (1) has a complex structure and omits the transient effect of the friction. It is more suitable in a simulation environment. The lumped parameter Modified-LuGre model has the form

$$\dot{z}_x(t) = v_{rx}\bar{f} - \frac{rw}{L_t}\delta z_x(t, L_t) - \theta\varphi(v_r)z_x(t) \quad (3)$$

for longitudinal direction, where $\varphi(v_r) = \frac{\hat{\sigma}_0\gamma(v_r)}{\mu_{kx}^2(v_r)}$. It is the average dynamics of the tire elasticity. z_x represents the mean of the tire tread deflection and δz_x is the trailing edge effect term of the contact patch on the average dynamics. The friction force is composed of three parts: force due to elasticity, force due to damping and force due to viscous-damping, i.e.

$$\begin{aligned} F_f &= \sigma_0 L_t z_x + \sigma_1 L_t \dot{z}_x + \sigma_2 v_{rx} F_n \\ &\approx \sigma_0 L_t z_x \end{aligned} \quad (4)$$

The first term in the friction force is the dominant term in the range of v_{rx}. This is the range we are interested in for this tire dynamics study.

The Modified-LuGre tire model uses μ_{kx}, μ_{ky} to represent the nominal surface 2D friction coefficients at a given slip. To capture the different surface conditions, from dry to icy, an additional parameter θ is introduced. In model (1) and (3), θ is the surface condition parameter. For a physical surface, the specific quantity of θ can be found to represent the tire friction but its value is not able to be measured in real time.

Thus, an adaptive mechanism is needed in the control design phase to estimate θ.

III. Desired Slip generation

A normalized control, $u_M \in [-1, 1]$, is used for the yaw moment controller, $|u_M| = 1$ for maximum yaw moment and $|u_M| < 1$ in a regular yaw moment generation. It leaves the freedom of determining the optimal yaw moment to the wheel level controller.

In this paper, a Pure Yaw Moment Control is designed based on assumptions on in-wheel-motor electric drive that (1) The longitudinal friction force can be generated independently on each individual wheel, (2) Braking torque and traction torque can be applied independently by two in wheel electric motors.

It implies the desired optimum slip ratios λ^* on the two sides of tires have same magnitudes but opposite directions so only the magnitude is calculated. This paper uses the rear axle moment M_r as the design example.

A. Maximum Yaw Moment Generation

When $|u_M| = 1$, the maximum yaw moment is desired. The contribution of each individual wheel on the yaw moment is a combination of F_x, F_y, e.g. $M_r(\alpha_r) = M_{xr}(\lambda, \alpha_r) + M_{yr}(\lambda, \alpha_r)$, $M_{xr}(\lambda, \alpha_r) = F_{xr}(\lambda, \alpha_r)Ab$, $M_{yr}(\lambda, \alpha_r) = F_{yr}(\lambda, \alpha_r)l_r$, where Ab is the axle based and l_r is the distance from vehicle CG to the rear axle. The lateral friction force $F_{yr}(\lambda, \alpha_r)$ is determined by vehicle lateral states (β, r), which are determined by the driver's intention or the tracking control requirement. The yaw moment is limited by physical capacity of tires on a specific surface condition, i.e. $M \in [-M_{\max}(\theta), M_{\max}(\theta)]$. Since F_y is determined mainly in vehicle control level by the steering input, determining the maximum of F_x is the key to find the optimum yaw moment M^*.

F_x is determined by the tire slip ratio λ. This slip control problem, however, is different from the one in an ABS or Traction control problem since F_x is reduced at the presence of the lateral friction force. The 2D tire friction force is determined by an ellipsoid force distribution associated with 2D motion.

By taking into account the tire traction capacity in both directions, the optimal problem of generating the maximum yaw moment on one axle reduces to finding λ^* for given α_r so that the generated differential friction has the largest yaw moment, i.e.

$$\max_{\lambda} M_r(\alpha_r) = \max_{\lambda}(F_{xr}(\lambda, \alpha_r)Ab + F_{yr}(\lambda, \alpha_r)l_r) \quad (5)$$

or

$$\lambda^* = \arg\max_{\lambda}(F_{xr}(\lambda, \alpha_r)Ab + F_{yr}(\lambda, \alpha_r)l_r) \quad (6)$$

Since F_{xr}, F_{yr} are continuous functions of λ, the necessary condition of the maximum M_r is

$$\frac{dM_r}{d\lambda} = \frac{dF_{xr}(\alpha_r)}{d\lambda}Ab + \frac{dF_{yr}(\alpha_r)}{d\lambda}l_r = 0 \quad (7)$$

Equation (7) gives a necessary condition of λ^*. It is straightforward to see that the maximum of M_r is achieved if and only if the increase of moment due to F_{xr} is equal to the decrease due to F_{yr}.

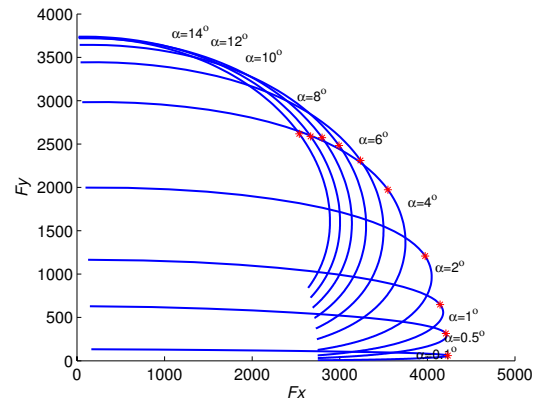

Fig. 3. 2D friction distribution on a tire at given slip angles with Maximum Moment Point marked

The 2D tire model (1) generates a friction force ellipse for a fixed α, as shown in Figure 3, when λ varies. The fixed α in the plot are $0.1°, 0.5°, 1°, 2°, 4°, 6°, 8°, 10°, 12°, 14°$ respectively. Figure 4 plots the generated friction force F_x, F_y as a function of λ at the specified αs.

The maximum are obtained directly by searching through λ, $\lambda \in [0, 1]$. The stars on each curve correspond to the optimum slip ratio λ^*s for the specific αs, $\lambda^* = [9.6\%, 9.1\%, 8.6\%, 9.1\%, 10.6\%, 13.1\%, 15.6\%, 18.1\%, 21.1\%, 23.6\%]$ in the case of the given αs.

It is observed that each $F_x(\lambda^*)$ is smaller than the maximum at the given α. The larger is α, the larger this discrepancy is. It implies that the optimum λ^* for the maximum yaw moment introduces less longitudinal friction than the maximum generated in ABS or Traction control systems. Therefore, an accurate tire slip ratio control is highly desired to achieve the optimal tire traction in the

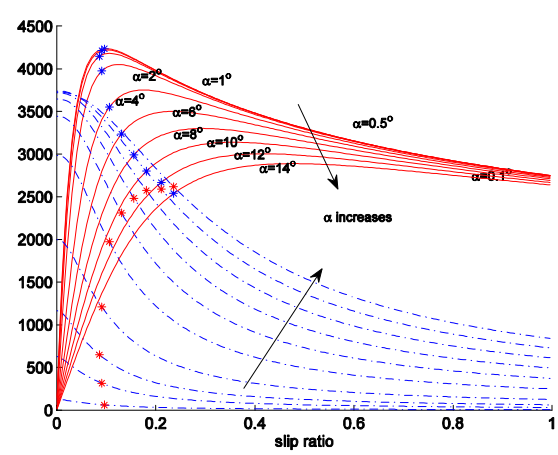

Fig. 4. Generated moment with respect to λ at given α (F_x: Solid, F_y: dash-dot)

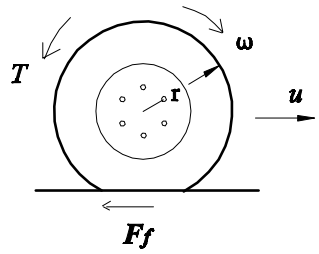

Fig. 5. Diagram of the model for slip control

stability control scenario.

B. Mapping from M_{xd} to λ_d

When $|u_M| < 1$, only partial of the maximum yaw moment is desired. The desired slip λ_d should be lower than the λ^* that we just derived, $\lambda_d = \rho\lambda^*$, $|\rho| < 1$. By (3), it is known that in the steady state

$$z_x = \frac{1}{\theta\varphi(v_r)}(v_{rx}f_n - \frac{rw}{L_t}z_L) \tag{8}$$

and since $v_{rx} = V_x\lambda$, the direct yaw moment can be found to be a function of λ in the steady state

$$\begin{aligned} M_x(\lambda) &= F_x Ab \\ &= \frac{\sigma_0 AbL_t}{\theta\varphi(v_r)}(V_x\lambda f_n - \frac{rw}{L_t}z_L) \end{aligned} \tag{9}$$

Equation (9) is a nonlinear relationship between the achieved slip ratio and the generated yaw moment. The inverse function $\lambda(M_x)$ does not have an analytical solution. Therefore, to generate an appropriate slip ratio command, a table of the nonlinear mapping between λ and M_x is derived then λ_d is derived by interpolating the generated table by command M_{xd}.

IV. Adaptive Tire Slip control

To achieve the slip ratio λ^*, an accurate braking/traction torque control is needed. Slip control is a challenging task in vehicle dynamics study due to the difficulty of accurately measuring vehicle speed V and the uncertainty of tire parameters as well as surface conditions. A nonlinear adaptive slip controller to surface conditions has been proposed in [4], [9]. But it is hard to extend such type of control to either a 2D case or to differential slip control. This study also uses a nonlinear control structure to drive the wheel slip ratio $\lambda \to \lambda_d$ with an adaptive mechanism to identify the surface condition. Figure 5 shows the relationship between friction force and brake torque on a wheel, where $u = V_x$ represent wheel longitudinal speed.

Here an additional measurement of wheel acceleration is used to solve the difficulty induced by the trailing edge effect term $\delta z_x(t, L_t)$ in (3). The control assume $F_{fl} = -F_{fr}$ thus the vehicle speed is not affected. The 2nd-order wheel dynamics in a braking scenario can be modeled by

$$J_\omega\dot{\omega}(t) = rF_f(t) - T(t) \tag{10a}$$

$$\dot{z}_x(t) = v_{rx}\bar{f} - \frac{rw}{L_t}\delta z_x(t, L_t) - \theta\varphi(v_r)z_x(t) \tag{10b}$$

and

$$F_f = \sigma_0 L_t z_x \tag{11}$$

Approximation is used in the previous equation for the friction force since the term $\sigma_0 L_t z_x$ dominates F_f in the slip control problem. The term $\delta z_x(t, L_t)$ can not be measured but it is known that

$$0 < \delta z_L(t) < z_L(V_x, \omega),\ t \in (0, \infty) \tag{12}$$

where $z_L(V_x, \omega)$ is a known function.

Model (10b) captures the nonlinear transient of the tire tread deflection with respect to the increase of the relative slip speed v_{rx}. When $|v_{rx}|$ is close to zero, $\varphi(v_r)$ is small so the dynamics of z_x is relatively "slow". As v_{rx} increases, the dynamics are faster so z_x can converge to the steady state quickly. In this study, the slip control is of interest thus the dynamics of the friction is important and the transient effect of z_x can not be omitted.

The wheel rotation speed ω and acceleration $\dot{\omega} = a_\omega$ are the only measurements and the torque applied to the wheel is the control variable. The tire slip ratio has the form

$$\lambda = \frac{u - rw}{u} = \frac{v_{rx}}{u} \tag{13}$$

in brake events and u is assumed to be constant here. The control goal of this problem is to drive $\lambda \to \lambda_d$ or equivalently if we define a target surface

$$s = v_{rx} - \lambda_d u \tag{14}$$

the control goal is to design a control to drive $s \to 0$. Since θ is not measured directly, an estimator $\hat{\theta}$ is introduced here and the error of the estimation is

$$\tilde{\theta} = \theta - \hat{\theta} \tag{15}$$

The way of constructing the estimator $\hat{\theta}$ will be introduced in the following derivation. θ varies much slower than the transient of this controlled system thus $\dot{\theta}$ can be omitted. Therefore,

$$\dot{\tilde{\theta}} = -\dot{\hat{\theta}} \tag{16}$$

The dynamics of the slip error is obtained by differentiating equation (14) and it has the form

$$\dot{s} = \dot{v}_{rx} = -r\dot{\omega} = -\frac{r}{J_\omega}(r\sigma_0 L_t z_x - T) \tag{17}$$

A nonlinear 2nd-order estimator is designed to be

$$\dot{\hat{\omega}} = \frac{r\sigma_0 L_t}{J_\omega}\hat{z} - \frac{1}{J_\omega}T \tag{18a}$$

$$\dot{\hat{z}}_x = v_{rx}\bar{f} - \frac{rw}{L_t}\delta\hat{z}_L - \hat{\theta}\varphi(v_r)\hat{z}_x + \mathcal{D} \tag{18b}$$

The form of $\delta\hat{z}_L$ and $\mathcal{D}$ terms will be determined subsequently.

Define the estimation error

$$\tilde{z}_x = z_x - \hat{z}_x \tag{19}$$

Then

$$\dot{\tilde{z}}_x = \frac{rw}{L_t}(\delta\hat{z}_L - \delta z_L) - \tilde{\theta}\varphi(v_r)\hat{z}_x - \theta\varphi(v_r)\tilde{z}_x - \mathcal{D}$$

The control task here is to drive $s \to 0$, $\tilde{z}_x \to 0$ and $\tilde{\theta} \to 0$ asymptotically so that the slip control task is achieved with the correct identification of surface condition. Choosing a Lyapunov function to be

$$V_{Lyap} = \frac{1}{2}s^2 + \frac{1}{2}\tilde{z}_x^2 + \frac{1}{2}\tilde{\theta}^2 \tag{20}$$

Then

$$\begin{aligned}\dot{V}_{Lyap} &= s\dot{s} + \tilde{z}_x\dot{\tilde{z}}_x + \tilde{\theta}\dot{\tilde{\theta}} \\ &= s(-\frac{r^2}{J_\omega}\sigma_0 L_t\hat{z}_x + \frac{r}{J_\omega}T) + \tilde{z}_x[-s\frac{r^2}{J_\omega}\sigma_0 L_t \\ &\quad +\frac{rw}{L_t}(\delta\hat{z}_L - \delta z_L) - \theta\varphi(v_r)\tilde{z}_x - \mathcal{D}] \\ &\quad -\tilde{\theta}[\dot{\hat{\theta}} + \tilde{z}_x\varphi(v_r)\hat{z}_x]\end{aligned}$$

To cancel out the last term in the expression of $\dot{V}_{Lyap}$, let the adaptive mechanism take the form

$$\dot{\hat{\theta}} = -\tilde{z}_x\varphi(v_r)\hat{z}_x \tag{21}$$

and the control braking torque be

$$T = r\sigma_0 L_t\hat{z}_x - \frac{J_\omega}{r}a_s s \tag{22}$$

where the arbitrary constant $a_s > 0$. Then we choose the driving term $\mathcal{D}$ to be

$$\mathcal{D} = -s\frac{r^2}{J_\omega}\sigma_0 L_t + \alpha_z\tilde{z}_x \tag{23}$$

where $\alpha_z > 0$ is a constant that can be tuned based on the control performance. Thus

$$\dot{V}_{Lyap} \le -a_s s^2 - (\theta\varphi(v_r) + \alpha_z)\tilde{z}_x^2 + \frac{rw}{L_t}\tilde{z}_x(\delta\hat{z}_L - \delta z_L) \tag{24}$$

On the right side of the inequality, the first two terms are negative definite while the last term is uncertain. It contains both the error term $\tilde{z}$ and the error term of the end-edge effect. To make it negative, the sign of $\tilde{z}$ has to be known.

In this estimator design, we use the error between the measured wheel rotational acceleration a_ω and the estimation as an index of estimator performance. Since we know the measurement of wheel acceleration $\dot{\omega} = a_\omega$, the error $\tilde{\omega} = \omega - \hat{\omega}$ is governed by the following dynamics

$$\dot{\tilde{\omega}} = \frac{r}{J_\omega}\sigma_0 L_t\tilde{z} = a_\omega - \frac{r\sigma_{0L_t}}{J_\omega}\hat{z}_x + \frac{1}{J_\omega}T \tag{25}$$

and thus

$$\tilde{z} = \frac{J_\omega}{r\sigma_0 L_t}a_\omega + \frac{1}{r\sigma_0 L_t}T - \hat{z}_x \tag{26}$$

It shows that the estimation error $\tilde{z}$ can be calculated by the measurement a_ω and the estimation $\hat{z}$.

To force the last term on the right side of (24) to be negative, let

$$\delta\hat{z}_L = \begin{cases} 0, & \tilde{z} > 0 \\ z_L(u,\omega), & \tilde{z} \le 0 \end{cases} \tag{27}$$

thus

$$\dot{V}_{Lyap} \le -a_s s^2 - (\theta\varphi(v_r) + \alpha_z)\tilde{z}^2 - \frac{rw}{L_t}|\tilde{z}|\, z_L \le 0 \tag{28}$$

By Lasalle's theorem, it can be concluded that

$$s \to 0,\ \tilde{z} \to 0,\ \text{as } t \to \infty$$

or

$$\lambda \to \lambda_d \text{ as } t \to \infty$$

The estimator dynamics of $\tilde{z}$ shows the following properties:

- $\mathcal{D} \to 0$ as $s \to 0$, $\tilde{z} \to 0$
- $\dot{\tilde{z}} < 0$ when $\tilde{z} = 0$ if $\tilde{\theta}\varphi(v_r)\hat{z} \neq 0$

The second property implies that

$$\tilde{\theta} \to 0,\ \text{as } t \to \infty$$

for $\hat{z} \neq 0$. Therefore, the discussion is based on an assumption that there is no such condition that

$$\hat{z}_x(t) \equiv 0 \text{ for all } t \in [t_0, t_0 + T] \tag{29}$$

or in other word if $\hat{z}_x(t)$ satisfies the following relationship for any time interval T

$$\frac{1}{T}\int_{t_0}^{t_0+T}\hat{z}_x^2(t)dt \geqslant a_0 > 0 \tag{30}$$

Condition (30) is a sufficient condition for the validity of the adaptive control and it implies persistent exciting of $\hat{z}_x(t)$. Intuitively, the adaptive mechanism needs to have the brake torque applied on the tire to generate z_x and $\hat{z}_x$ to guarantee $\tilde{\theta}'$s convergent.

V. Simulation

A simulation model is set up in MATLAB Simulink to verify the control design on various surface conditions. Estimation $\hat{\theta}$ from the slip controller is feedback into the slip generator to take into account the surface friction coefficient on the desired slip ratio λ_d. To eliminate the high frequency noise in $\hat{\theta}$, a Butterworth low-pass filter with cut-off frequency at 10 rad/s is used in the simulation.

The left figure in Figure 6 plots the transient of $\hat{\theta}$ with respect to time responding to the real surface variation $\theta(t)$. $\theta(t)$ is given as a ramp function in this simulation. The right figure in Figure 6 shows the achieved λ with respect to the command λ_d under the given $\theta(t)$. It shows the estimation of θ is fast with small offset. Since $|\theta| \ge 1$ in the tire model, the controller will ignore any estimation that is less than 1. Thus, a flat λ_d corresponding to $\theta = 1$ is observed at the beginning. After an effective $\hat{\theta}$ is obtained from the feedback, λ_d is decreased accordingly. Overall, the achieved λ has very good tracking of λ_d in this simulation.

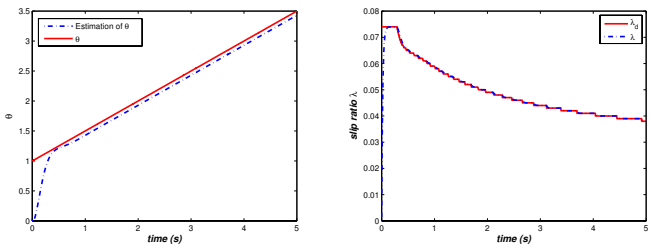

Fig. 6. θ vs $\hat{\theta}$ (left) and λ_d vs λ (right) in the transient

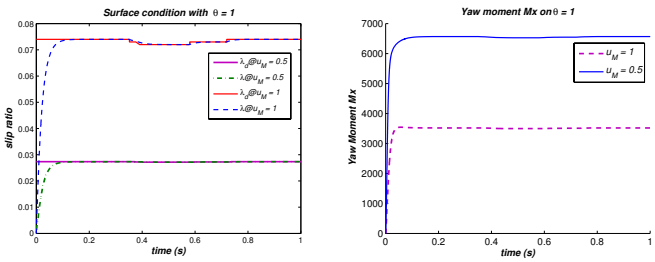

Fig. 7. Achieved λ and M_x at $\theta = 1$

Figure 7 to Figure 8 plot the achieved λ and M_x at $\theta = 1$ and $\theta = 2$ when $u_M = 1$ and $u_M = 0.5$ are commanded.

In Figure 7, a good surface condition with $\theta = 1$ is simulated. The left plot shows λ_d and λ under demands for full yaw moment and half yaw moment on surface. The generated M_x are shown in the right plot.

In Figure 8, a slippery surface condition with $\theta = 2$ is simulated. In the left plot, it is shown that the slip generator reduces λ_d after obtaining the feedback information of $\hat{\theta}$. The slip controller successfully regulates λ to λ_d in the steady state with a fast transient.

From the right plot of Figure 7 to Figure 8, one can also observed that with the command of $u_M = 1$ and $u_M = 0.5$, the achieved yaw moment keeps a linear relationship as required by u_M while the steady state slip ratios are in a nonlinear form.

VI. CONCLUSIONS

This study makes a connection between the vehicle level yaw moment controller and the wheel-tire level slip control. It generates a normalized yaw moment command to the lower level wheel controller. The lower level controller generates either the optimal tire slip ratio for the yaw moment or a slip ratio based on a nonlinear slip-to-yaw moment map. It shows that the optimal slip ratio for the maximum yaw moment generation is not the slip quantity corresponding to the maximum longitudinal friction force. This result explains the importance of considering the effect of lateral deflection of the tire in the yaw moment control design. The designed controller is adaptive to the surface friction condition modeled by a parameter in the tire model. The slip generator uses the estimated surface parameter to make adaptive generation to the surface condition. The designed controller has been tested in a simulation model. Both the slip ratio and surface estimation converge to the real value under the adaptive controller.

Further work of this study includes implementation of the designed lower level controller with vehicle controllers and studies of the slip control mechanism when the vehicle speed varies due to non-uniform friction generation on each tire.

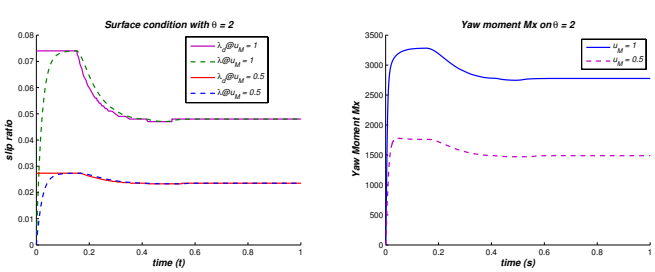

Fig. 8. Achieved λ and M_x at $\theta = 2$

REFERENCES

[1] M. Abe, N. Ohkubo, and Y. Kano, "A direct yaw moment control for improving limit performance of vehicle handling - comparision and cooperation with 4ws," *Vehicle System Dynamics*, vol. 25, pp. 3–23, 1996.

[2] ——, "A direct yaw moment control for improving limit performance of vehicle handling - comparison and cooperation with 4ws," *Vehicle System Dynamics*, vol. Supplement 25, pp. 3–23, 1996.

[3] M. Canale, L. Fagiano, M. Milanese, and P. Borodani, "Robust vehicle yaw control using active differential and internal model control techniques," in *Proceedings of the 2006 American Control Conference*, Minneapolis, Minnesota, June 2006.

[4] C. C. de Wit and R. Horowitz, "Observers for tire/road contact friction using only wheel augular velocity information," in *Proceedings of 38th IEEE Conference of Decision and Control*, Phoenix, Arizona, December 1999.

[5] W. Liang, J. Medanic, and R. Ruhl, "An analytical dynamic tire model," *Vehicle System Dynamics*, vol. 46, no. 3, pp. 197–227, March 2008.

[6] W. Liang, "Lateral tracking and stability control for automated vehicles," Ph.D. dissertation, University of Illinois at Urbana-Champaign, 2007.

[7] H. Tseng, B. Ashrafi, D. Madau, B. Allen, T. Brown, and D. Recker, "The development of vehicle stability control at ford," *IEEE/ASME Transactions on Mechatronics*, vol. 4, no. 3, pp. 223–234, Sep 1999.

[8] K. Wakamatsu, Y. Akuta, M. Ikegaya, and N. Asanuma, "Adaptive yaw rate feedback 4ws with tire/road friction coefficient estimator," *Vehicle System Dynamics*, vol. 27, pp. 305–326, 1997.

[9] J. Yi, L. Alvarez, X. Claeys, and R. Horowitz, "Emergency braking control with an observer-based dynamic tire/road friction model and wheel angular velocity measurement," *Vehicle System Dynamics*, vol. 39, no. 2, pp. 81–97, 2003.

[10] H. Yu, W. Liang, R. McGee, and M. Kuang, "Vehicle handling assistant control system vis independent rear axle torque biasing," in *American Control Conference*, 2009.